Charge-switchable molecular magnet and spin blockade of tunneling

C. Romeike,[1] M. R. Wegewijs,[1] M. Ruben,[2] W. Wenzel,[2] and H. Schoeller[1]
[1]*Institut für Theoretische Physik A, RWTH Aachen, 52056 Aachen, Germany*
[2]*Institut für Nanotechnologie, Forschungszentrum Karlsruhe, 76021 Karlsruhe, Germany*
(Received 10 December 2004; revised manuscript received 5 July 2006; published 5 February 2007)

We analyze a model for a metal-organic complex with redox orbitals centered at both the constituent metal ions and ligands. We focus on the case where electrons added to the molecule go onto the ligands and the charge fluctuations on the metal ions remain small due to the relatively strong Coulomb repulsion. Importantly, if a nonzero spin is present on each metal ion it couples to the intramolecular transfer of the excess electrons between ligand orbitals. We find that around special electron fillings, addition of a single electron switches the total spin $S_{\mathrm{tot}}=0$ to the maximal value supported by electrons added to the ligands, $S_{\mathrm{tot}}=3/2$ or even $S_{\mathrm{tot}}=7/2$ for metal ions with spin 1/2. This charge sensitivity of the molecular spin is a strong correlation effect due to the Nagaoka mechanism. Fingerprints of the maximal spin states, as either ground states or low-lying excitations, can be experimentally observed in transport spectroscopy as spin blockade at low bias voltage and negative differential conductance and complete current suppression at finite bias, respectively.

DOI: 10.1103/PhysRevB.75.064404 PACS number(s): 75.50.Xx, 73.23.Hk, 31.25.Qm, 71.10.Fd

I. INTRODUCTION

Recent experiments on metal-organic grid complexes, consisting of rationally designed ligands and metal ions as building units, have exhibited interesting electrochemical,[1–3] magnetic,[4–7] and transport properties.[8] By self-assembly the metal ions and ligands arrange in a rigid, highly symmetric grid (see Fig. 1). Due to their different nature, electron orbitals can often be roughly attributed to either the metal ions or the ligands. Such a separation has been used successfully to describe the low-temperature intramolecular spin coupling of Co-$[2\times2]$ grids[9,10] and Mn-$[3\times3]$ grids[5–7] for a fixed charge state as well as the electrochemical properties of (Mn,Fe,Co,Zn)-$[2\times2]$ (Refs. 11–13) and Mn-$[3\times3]$ grids[2] and scanning tunneling microscopy (STM) measurements on a Co-$[2\times2]$ grid.[8] For such complexes it is well known[14] that both the pyridine ligands as well as the metal ions can be reduced. Which type of redox site is preferred depends on chemical details which can be controlled, mainly by substitution of metal ions and modification of the ligand.[11] This raises the interesting question of whether magnetic states can be associated with extra electrons added to the ligands. Another question concerns the effect of the motion of the excess electrons[15] on different equivalent redox sites. Finally, the observation of high-spin states in three-terminal transport experiments on single molecules[16–25] is of interest. In such a setup, the number of electrons on the molecule can be controlled electrostatically with a gate voltage, which opens up the possibility of single-molecule spin switching. In addition, the bias voltage induces a current which is sensitive to the spin.

Here we analyze a phenomenological low-temperature model for a $[2\times2]$ grid molecule consisting of four ligands "holding" either four metal zero-spin ions (Fe grid) or four spin-1/2 ions (Co grid). This is sketched in Fig. 2. We show that (i) the molecular spin can be highly sensitive to the charge added to the ligands and can therefore be switched electrically, (ii) if open-shell metal ions are present between the ligands their spin degrees of freedom may also be switched, and (iii) the spin splitting gives rise to clear fingerprints in tunneling spectroscopy due to spin blockade physics. For the particular geometry and connectivity of the redox orbitals in a $[2\times2]$ grid, the Nagaoka mechanism[26] becomes effective, but only for special numbers of added electrons. Due to the strong electrostatic interaction the delocalization of an extra hole or electron (relative to half filling) favors a fully polarized background of all other electrons. This may dominate over the antiferromagnetic superexchange processes. In the context of band magnetism the relevance of the Nagaoka mechanism is limited due to its lattice-type dependence[27] and its strong charge sensitivity. Only for a single additional electron or hole relative to a half-filled band can the spin-polarization effect be guaranteed. In single-molecule devices, however, the strong charge sensitivity is of great interest, since the issues of the control of the charge and the geometry can be overcome. First, the advanced rational design of supramolecular structures allows complex "lattice" types to be realized.[1,28] Second, due to the energy and charge quantization one can modulate the total charge of a molecule by a single electron.[16–25]

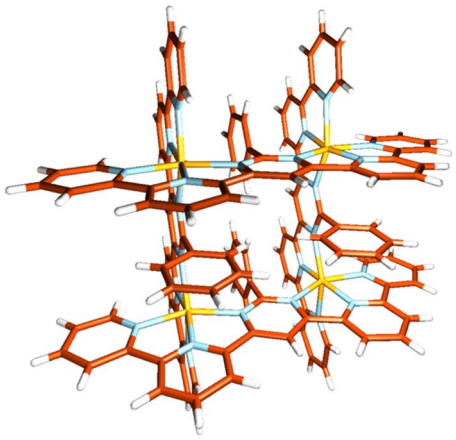

FIG. 1. (Color online) Structure of the $[2\times2]$-grid-type complex.

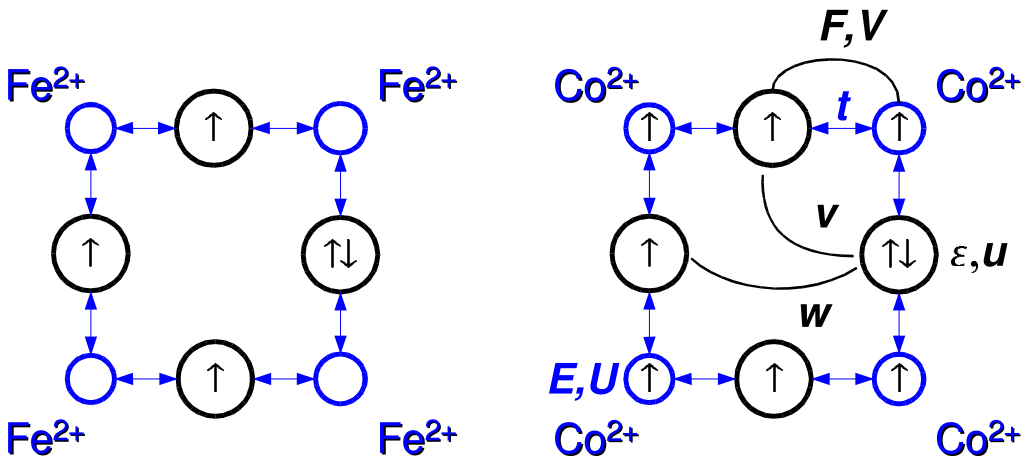

FIG. 2. (Color online) Grid molecule: small (large) circles represent metal-ion (ligand) orbitals.

In this paper we show that sufficiently strong short-range interaction on the ligands (relative to the ligand-ion tunneling) increases the ground-state spin from $S_{\mathrm{tot}}=0$ to the maximal value supported by three (or five) extra electrons on the molecule, $S_{\mathrm{tot}}=3/2$ for the Fe grid, and $S_{\mathrm{tot}}=7/2$ for the Co grid. The spin properties of the molecule can thus be controlled electrically.[29–31] In single-electron tunneling transport this high-spin ground state leads to spin blockade at low bias voltage.[32] In addition, even for a low-lying maximal spin excitation negative differential conductance (NDC) effects and complete current suppression at finite bias voltage occur. Here we link such transport fingerprints to the Nagaoka effect and the spin-excitation spectrum of the grid in adjacent charge states. We note that the transport effects of magnetic states[20,22] were recently predicted to give rise to rich transport signatures even for the most simple spin-Hamiltonian models[33,34] taking into account magnetic anisotropy in a single-spin S multiplet. Here we focus on effects related to different spin multiplets with energy separation much larger than the magnetic anisotropy splittings which we neglect. We emphasize that the situation considered here is different from that in the STM experiment in Ref. 8 where the transport is due to electron extraction from metal ions in the grid. Here we consider the case where the electrostatic environment and the modified ligands favor electron addition to the complex by reduction of ligands, which has been observed in a number of electrochemical experiments. Also, in the three-terminal device discussed here the more symmetric coupling leads to pronounced nonequilibrium effects.

We will first discuss the model (Sec. II) and the resulting energy and spin spectra (Sec. III). For an illustrative case we discuss the transport in detail (Sec. IV).

II. MODEL

We consider a model of a grid complex with four metal and four ligand sites. The simplest model capturing the physics of interest takes into account one orbital per site (Fig. 2). For a grid complex the local symmetry of the ligand field at a metal ion typically is lower than octahedral so that the extra electron in a Co^{2+} ion (with respect to Fe^{2+}) occupies a nondegenerate orbital. We assume that this electron-accepting d orbital is separated energetically from ligand orbitals. Each metal-ion orbital which we account for is thus either unoccupied (Fe grid) or occupied (Co grid) and carries a spin 0 (Fe grid) or 1/2 (Co grid). The Coulomb repulsion on the ions is typically much stronger than on the ligands. Therefore the charge on each ion is fixed, but their spin degree of freedom has to be kept. In contrast, on the ligands only the total number of electrons is fixed while charge rearrangements remain possible that involve tunneling across the intermediate metal ions, which carry a spin in the case of the Co-grid model. This is the basic physics that we want to investigate. The following Hamiltonian captures the features of the electronic degrees of freedom:

$$H = H_{\mathrm{T}} + H_{\mathrm{L}} + H_{\mathrm{Fe/Co}} + H_{\mathrm{dir}} + H_{\mathrm{V}}, \tag{1}$$

$$H_{\mathrm{T}} = \sum_{\langle i,j\rangle} \sum_{\sigma} t A^{\dagger}_{i,\sigma} a_{j,\sigma} + \mathrm{H.c.}, \tag{2}$$

$$H_{\mathrm{L}} = \sum_{j=1}^{4} (\epsilon n_j + u n_{j,\uparrow} n_{j,\downarrow} + v n_j n_{j+1}) + w \sum_{j=1}^{2} n_j n_{j+2}, \tag{3}$$

$$H_{\mathrm{Fe/Co}} = \sum_{i=1}^{4} (E N_i + U N_{i,\uparrow} N_{i,\downarrow}), \tag{4}$$

$$H_{\mathrm{dir}} = -2F \sum_{\langle i,j\rangle} \left(\mathbf{S}_i \mathbf{s}_{j,j} + \frac{1}{4} N_i n_j \right), \tag{5}$$

$$H_{\mathrm{V}} = V \sum_{\langle i,j\rangle} N_i n_j. \tag{6}$$

In Fig. 2 all interactions in the model are schematically indicated. Operators and variables (except t) in lower (upper case) relate to the ligand (metal ion) and all indices run from 1 to 4 cyclically. $\langle i,j\rangle$ denotes a summation over neighboring metal ions i and ligands j. The operator $a^{\dagger}_{j\sigma}$ creates an electron on ligand site j with spin σ, $n_{j\sigma}=a^{\dagger}_{j\sigma}a_{j\sigma}$, and $n_j=\Sigma_{\sigma} n_{j\sigma}$. Similar definitions hold for the metal ions: $A_{i\sigma}$, $N_{i\sigma}=A^{\dagger}_{i\sigma}A_{i\sigma}$, $N_i=\Sigma_{\sigma} N_{i\sigma}$. $\mathbf{S}_i$ is the electron spin of metal ion i and $\mathbf{s}_{j,k}$

$=\frac{1}{2}\Sigma_{\sigma,\sigma'}a^{\dagger}_{j,\sigma}\boldsymbol{\tau}_{\sigma,\sigma'}a_{k,\sigma'}$ is an operator related to the ligands, where $\boldsymbol{\tau}$ is the vector of Pauli matrices. term (2) describes hopping between the ligands and metal ions ($t<0$) and is assumed to be independent of i and j due to molecular symmetry. The ligand part of the Hamiltonian (3) consists of an orbital with energy ϵ and the Coulomb repulsion terms on the ligand (u) and between adjacent (v) and opposite ligands (w). The charging energies associated with the reduction of ligand orbitals were reported in cyclic voltammetry experiments.[11] Due to decreasing overlap with distance we have $u>v/2\geqslant w$ [e.g., for Fe^{2+} $u\approx 4v\approx 2w\approx 0.3$ eV (Ref. 11)]. The Hamiltonian (4) describes the metal ion orbitals with energy E. Here we only consider the short-range interaction U because the d-orbital overlap between two ions is typically much smaller than that between two ligand orbitals. In order to describe the coupling of electron spins on the metal ions and ligands in a balanced way, we must include a direct exchange interaction (5) with $F>0$. This stabilizes ferromagnetic states even when it is weak[35] (see Sec. III below). For consistency the metal-ligand charging energy (6) also needs to be incorporated: in general $F\lesssim V$ are of the same order. However, in the regime of interest the particle number on each metal ion is fixed ($N_i=0$ for an Fe grid, $N_i=1$ for a Co grid), so the second term in (5) and (6) yields a constant.

We study the parameter regime where the first eight extra electrons occupy four equivalent ligand-centered orbitals. Such a sequence has been well documented in electrochemistry experiments for a number of grid molecules.[11] For an Fe grid we must then assume that the two charge states of the ligand lie below the metal-ion orbital energy E:

$$\epsilon < \epsilon + u < E < E + U \quad \text{(Fe grid)}. \tag{7}$$

For a Co grid the two charge states of the ligand lie between the singly and doubly occupied states of the metal ion:

$$E < \epsilon < \epsilon + u < E + U \quad \text{(Co grid)}. \tag{8}$$

The orbital energy difference $\Delta=\epsilon-E$ is associated with metal ion to ligand charge transfer (MLCT) between unoccupied metal-ion and ligand sites. In the case of an Fe grid $\Delta<0$ and in the case of a Co grid $\Delta>0$.

In the limit $|\Delta|\gg|t|$ (Fe grid) $[\Delta, U-\Delta\gg|t|$ (Co grid)] the charge transfer between ligands and metal ions is suppressed and some qualitative insight can be gained. The effect of the fluctuations of the orbital occupation around zero (Fe) or one (Co) can be incorporated in an effective tunnel coupling between the ligands using second-order Brillouin-Wigner perturbation theory (equivalent to a Schrieffer-Wolff transformation[36]). We thereby eliminate the charge degrees of freedom on the metal-ion sites. In the resulting effective model each metal-ion sites are thus either entirely eliminated (Fe) or characterized by a pure spin degree of freedom (Co). We are left with the effective Hamiltonian (up to a constant)

$$H^{\text{eff}}_{\text{Fe}} = \sum_{\langle jk\rangle}\sum_{\sigma} T a^{\dagger}_{j,\sigma}a_{k,\sigma} + H_{\text{L}}, \tag{9}$$

$$H^{\text{eff}}_{\text{Co}} = \sum_{i}\sum_{j,k=i,i+1}\left\{J\mathbf{S}_i\mathbf{s}_{j,k} + \sum_{\sigma} K a^{\dagger}_{j,\sigma}a_{k,\sigma}\right\} - \sum_{i}\sum_{j=i,i+1} F\mathbf{S}_i\mathbf{s}_{j,j} + H_{\text{L}}. \tag{10}$$

This model describes the low-energy properties of the mobile excess electrons on the grid. The coupling constants T, K, and J are

$$T=\frac{t^2}{2\Delta},$$

$$K=\frac{1}{2}\left(\frac{t^2}{\Delta}-\frac{t^2}{U-\Delta}\right),$$

$$J=\frac{1}{2}\left(\frac{t^2}{\Delta}+\frac{t^2}{U-\Delta}\right). \tag{11}$$

For an Fe grid the effective Hamiltonian is the extended Hubbard model on four ligand sites with effective hopping matrix element T. In contrast, for a Co grid we retain an eight-site model where the spin and charge on the four ligands are coupled to the pure spin on the four metal ions. The first two terms in (10) describe tunneling between ligands with (J) and without a spin flip (K), whereas the last two terms describe fluctuations of the charge and spin on the ligands. Equation (10) may be rewritten as $H^{\text{eff}}_{\text{Co}}=\Sigma_{\sigma,i}\Sigma_{j,k=i,i+1}\{(K+J\sigma S^{z}_{i})a^{\dagger}_{j,\sigma}a_{k,\sigma}+JS^{+\sigma}_{i}s^{-\sigma}_{j,k}+[K+(J-2F)\sigma S^{z}_{i}]n_{j,\sigma}+(J-2F)S^{+\sigma}_{i}s^{-\sigma}_{j,j}\}+H_{\text{L}}$. This makes explicit that electrons with spin σ (anti)parallel to the local spin $\mathbf{S}_i$ on the metal ion tunnel with amplitude $K\pm J$, where $J>|K|\geqslant 0$ and $K\gtrless 0$ for $\Delta\lesssim U/2$. Also, the direct ferromagnetic exchange ($F>0$) clearly counteracts the antiferromagnetic exchange coupling ($J>0$) between the ligand and metal-ion spins.

The interplay of kinetic and Coulomb-interaction effects of the extra electrons on the ligands gives rise to a nonstandard ferromagnetic spin coupling as will be discussed in the next section in detail. In particular, we point out that the effective Hamiltonian (10) for a Co grid contains no explicit interaction term between the metal-ion spins: all interactions are mediated by the electrons on the ligands. Since we want to describe transport involving these ligand electrons we cannot use an effective spin-Hamiltonian description here. In the absence of extra electrons on the ligands, a weak effective antiferromagnetic Heisenberg exchange interaction between the spins on the metal ions is mediated by an empty intermediate ligand orbital. A four-site Heisenberg model with this effective coupling has been studied in Ref. 9 and the results agree with the experiments on Co grids. However, this interaction appears only in fourth-order perturbation theory in the tunneling t. In our case the ligand orbitals contain one or more extra electrons and the weak fourth-order effect is superseded by the coupling, second order in t, incorporated in our effective Hamiltonian (10). We also note that low-density quantum dots, where electrons can be considered as localized in "pocket states," also exhibit high-spin states and their impact on transport has been considered.[37] Here, however, we also consider the effect of open-shell ions with nonzero spin

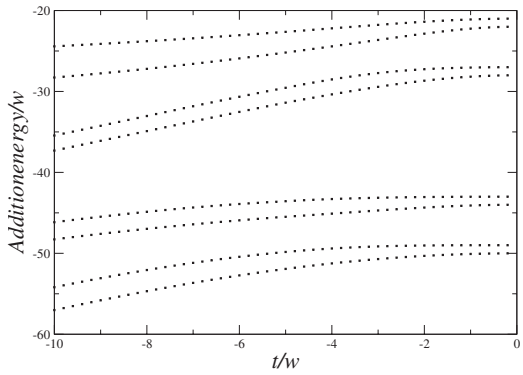

FIG. 3. Addition energy of Fe grid as a function of tunneling t (in units of w) for $u=15$, $v=3$, $w=1$, $\Delta=-50$, $U=100$ calculated from the full model (1). For $|t|<|\Delta|$ we are in the perturbative regime where no spin is localized on the Fe site and the effective model (9) applies. This type of addition energy spectrum was measured in electrochemical experiments (Ref. 11) and is also expected in transport spectroscopy where the size of the Coulomb diamonds is proportional to the spacings (see also Fig. 4).

which mediate the tunneling between the ligands. Such situations were also considered in the context of exotic Kondo effects involving dynamical symmetries in multiple quantum-dot systems.[38,39] Finally, similar models with two types of electron orbitals have been studied for the description of the neutral-ionic transition[40] in organic crystals, in the context of ferroelectrics and superconductivity in transition metal oxides.[41]

III. ADDITION ENERGIES AND SPIN STATES

We now present the results for the full Hamiltonian (1) and the effective Hamiltonians (9) and (10) (perturbation theory). We first study the addition energy spectra, which reflect mainly the electrostatic effects and then focus on the spin properties of the ground states and lowest-lying excited states as a function of the number of added electrons n.

A. Fe grid

To highlight the role of the electrostatic interactions, let us first discuss the noninteracting limit of the effective model (9) for an Fe grid ($u,v,w \ll |T|$). There are four doubly degenerate eigenstates: one lowest orbital state at energy $\epsilon-2|T|$, two orbitally degenerate states at ϵ (due to the fourfold symmetry axis), and the highest state at $\epsilon+2|T|$. The electron addition energy spectrum consists of a pair of twofold degenerate energies with a fourfold degenerate energy in between. The charging effects, which reflect the geometry of the grid, give rise to a qualitatively very different addition spectrum which can only be understood by including the interactions $u>v>w$ in our full and effective model. In Fig. 3 we plot the addition energies as a function of the tunneling amplitude t calculated for the full model for the Fe grid which is in qualitative agreement with the experiments.[11] The first electron reduces one of the four ligands. The next one goes onto the opposite ligand in order to minimize the Coulomb interaction. The third and fourth electrons reduce

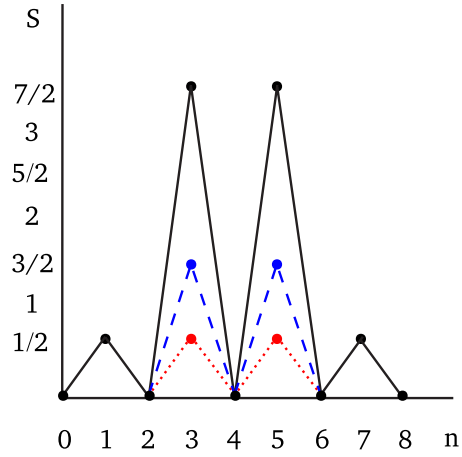

FIG. 4. (Color online) Ground-state spin as a function of the number of electrons n added to the ligands for $u>u_{\mathrm{th}}$ (dashed blue line, Fe grid; black line, Co grid) and for $u<u_{\mathrm{th}}$ (dotted red line in both cases).

the adjacent ligands. For the next four electrons this sequence of processes is repeated, each time doubly occupying a ligand orbital. We thus have two sets of four reduction peaks separated by a large gap of order u. Each set of four subdivides into two pairs of closely spaced peaks (distance w) separated by a moderate gap $2v-w<u$. The tunneling between equivalent ligands only weakly affects this picture when it is weak relative to the charging energies. Therefore from here on we express all energies in units of $|t|$.

Now we discuss the ground-state spin as successive electrons are added to the ligands using the effective model (9). We start again from the noninteracting case ($u,v,w \ll |T|$): filling the levels according to the Pauli principle we obtain a ground-state spin $S_{\mathrm{tot}}=1/2$ for odd particle number n. For even $n=2,6$ the ground-state spin is $S_{\mathrm{tot}}=0$, whereas for half filling ($n=4$) $S_{\mathrm{tot}}=0$ and $S_{\mathrm{tot}}=1$ are degenerate. The initial effect of increasing the interactions u, v, w from zero is to suppress the charge fluctuations: we obtain a Heisenberg antiferromagnet at $n=4$ with a singlet ground state for $u \gg |T|$ (Fig. 4).

However, for sufficiently large u beyond a threshold, $u>u_{\mathrm{th}}^{\mathrm{Fe}}$ (see Fig. 5), the ground-state spin for odd $n=3,5$ is enhanced from the noninteracting value $S_{\mathrm{tot}}=1/2$ to the maximal possible value $S_{\mathrm{tot}}=3/2$ (Fig. 4). Here the tunneling

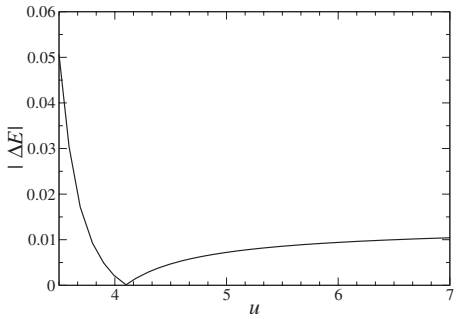

FIG. 5. Fe grid: Ground- to excited-state gap of the effective model as function of u for $n=3$, $\Delta=-10$, $v=2.25$, $w=1$. For $u>u_{\mathrm{th}} \approx 4.15$ the ground state has maximal spin.

between the ligands via the empty orbitals on the ions plays a decisive role: because double occupation is suppressed, a single hole or electron (relative to the half-filled state $n=4$) can maximally gain kinetic energy when the background of the other electrons is fully spin polarized. This ferromagnetic alignment is a many-particle effect which requires the exact diagonalization of the effective model. It competes with the antiferromagnetic spin coupling due to superexchange processes. Which process dominates depends on the strength of the on-site repulsion u relative to the hopping $|T|$, i.e., $u_{\mathrm{th}}^{\mathrm{Fe}} \propto |T|$. The absolute value of the gap $|\Delta E|$ between the maximal spin ground state and lowest excited state saturates at a value $\sim 2|T|$ with increasing u. This is in accordance with the kinetic origin of the effect: as soon as double occupation is suppressed the precise value of u becomes irrelevant. This is the mechanism underlying the Nagaoka theorem[26] which guarantees that the ground state has maximal spin if u is larger than some positive threshold value. It applies to the effective model (9) because it satisfies a certain connectivity condition for the lattice, namely, that a so-called exchange loop exists which is no longer than four sites.[27,42] For this mechanism to be relevant one should have both moderate effective hopping T (i.e., a sizable gap $|\Delta E|$) and strong on-site interaction u which seems achievable in weakly coupled supramolecular structures such as the grids considered here. The interaction u can be enhanced by a chemical modification of the ligands to draw charge density onto the ligand in the lowest unoccupied molecular orbitals. Taking typical parameters[11] $|\Delta| \approx 1$ eV, $|t| \approx 10^{-1}$ eV, we estimate $u_{\mathrm{th}}^{\mathrm{Fe}} \approx 4 \times 10^{-2}$ eV and the spin gap as $|\Delta E| \gtrsim 10^{-2}$ eV for $u > 5 \times 10^{-2}$ eV which is certainly resolvable in transport experiments.

We checked that localization of electrons counteracts the Nagaoka effect, which is expected due to its kinetic nature. For instance, increasing the interactions with neighboring sites v, w increases the threshold value $u_{\mathrm{th}}^{\mathrm{Fe}}$ for the Nagaoka state to a higher but finite value, (cf. Ref. 35). Similarly, we analyzed the effect of static disorder which is expected to be relatively weak since the ligands and the metal ions form a highly symmetric grid of equivalent centers. The Nagaoka state remains stable even if the ligand sites become inequivalent through different MLCT barriers $\Delta < |T|$.

B. Co grid

The charge addition energy spectrum which we obtain for the Co grid is qualitatively similar to that for the Fe grid since it is dominated by charging effects on the ligands. In the experiment[3] the first three reduction waves correspond to three one-electron reductions with nonequidistant spacing (0.04 and 0.150 eV, respectively), similar to those of Fe grids, and in agreement with the model considered here. However, the subsequent six one-electron reduction waves exhibit an enlarged but roughly constant spacing 0.24–0.33 eV. This may be compared to the charging of one big "island" with better screening and would require in our model an *ad hoc* change of the parameters to $u \approx v \approx w \approx 0.3$ eV for $n > 3$. Obviously, effects become important that are not included in our electronic low-temperature model, e.g., adding electrons could result in a change in the molecular geometry which will lead to different electrostatic interactions. Also, at the high experimental temperatures individual Co ions may be in the high-spin state where the d orbitals (approximate t_{2g} symmetry) are singly occupied. These can couple more strongly to the ligand orbitals (π symmetry) and increase metal-ligand charge transfer. Clearly, these complicated issues are beyond the scope of this paper: we are interested in the low-temperature regime and assume low-spin ($S=1/2$) Co ions.

The spin properties of the eigenstates of the effective model (10) require a discussion of the cooperative effect of the direct exchange and Nagaoka spin coupling. Let us first neglect the direct exchange interaction, i.e., $F=0$. Then the resulting spin spectrum is qualitatively similar to the Fe grid (Fig. 4). We have a singlet ground state at half filling ($n=4$), and a Nagaoka maximal spin ground state near half filling ($n=3,5$) for sufficiently large charging ($U > u > u_{\mathrm{th}}^{\mathrm{Co}}$). At half filling $n=4$ the antiferromagnetic Néel state has the largest weight in the ground state. The electron spins on the metal ions are aligned parallel due to the presence of electrons on the ligands and vice versa. (This is to be contrasted with the situation for the Fe grid at $n=4$, where the electron spins on adjacent ligands are aligned antiparallel.) The total spins of the metal-ion and ligand sublattices couple antiferromagnetically to a singlet ground state. The appearance of the Nagaoka state at $n=3,5$ has a different origin than in the Fe grid since we have exchange loops longer than four sites. In this case, however, we have a bipartite lattice (hopping occurs only between the ligand and metal-ion sublattices). This is also a sufficient condition for the Nagaoka theorem to apply.[27,35]

Two quantitative differences are introduced by the four spins on the bridging Co ions compared with the Fe grid. First, the maximal spin value attained in the Nagaoka state is more than twice larger, $S_{\mathrm{tot}}=7/2$. Second, the threshold value of $u_{\mathrm{th}}^{\mathrm{Co}}$ for the appearance of this state is dramatically increased, $u_{\mathrm{th}}^{\mathrm{Co}} \approx 10^4$ (in both the full and effective models). This is due to the antiferromagnetic exchange coupling J between the metal-ion and ligand sublattices (discussed at the end of this section). However, the neglect of any (even small) direct exchange represents an unbalanced treatment of the spin coupling, since the Nagaoka mechanism and the direct exchange are known to cooperate in the stabilization of maximal spin states.[35] Figure 6 shows that increasing the direct exchange leads to a dramatic reduction of the threshold Coulomb energy for achieving the Nagaoka state, reaching values of the same order as for the Fe grid, e.g., $u_{\mathrm{th}}^{\mathrm{Co}} \sim 5$ for $F \approx J$. Simultaneously the gap between ground and excited states increases, i.e., the high-spin state is stabilized. The excitation gap ΔE as a function of u (Figs. 6) saturates at values of the order of $0.2J$. In this limit the direct exchange "kicks"[35] the system into the Nagaoka state. The direct exchange may also induce a maximal spin state at half filling $n=4$. In this case the spin can only be switched from 0 to 7/2 when going from $n=2$ to 3 (or from $n=5$ to 6). For $F \gg J$ the resulting ground state always has maximal spin (even for $n=4$) independent of u, indicating that the Nagaoka mechanism is no longer relevant.

Now we discuss qualitatively the increase of u_{th} relative to the Fe-grid case due to the spins on the Co ions with the

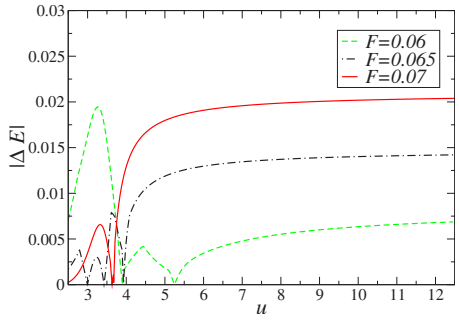

FIG. 6. (Color online) Co-[2×2] grid: Ground to excited-state gap for the effective model as a function of u for $n=3$, $\Delta=10$, $U=100$, $v=2.25$, $w=1$, and three different values for the direct exchange $F=0.06, 0.065, 0.07$. The nonmonotonic behavior of the gap is due to several level crossings until the Nagaoka state is the ground state (beyond the rightmost zero). The direct exchange "kicks" the system into the Nagaoka state: the threshold value $u_{\mathrm{th}}^{\mathrm{Co}}$ is reduced when $F \to J=0.06$. Even for smaller $F>0$ one still needs $u>u_{\mathrm{th}}^{\mathrm{Co}}$ to drive the system into the maximal spin ground state.

ligand electrons. We consider two extreme limits.

(i) If the sublattices are well separated in energy (Δ, $U-\Delta \gg |t|$), the effective model (10) applies. From the discussion following Eq. (10) it is evident that the antiferromagnetic coupling J opposes maximal spin states; hence $u_{\mathrm{th}}^{\mathrm{Co}}$ is increased. (ii) If the two sublattices are nearly equivalent ($\Delta, U-u \ll |t|$) we have to consider the full model. Nagaoka's mechanism is now ineffective because the exchange paths are longer than four sites.[27] This implies also a very large $u_{\mathrm{th}}^{\mathrm{Co}}$ to stabilize the Nagaoka state.

IV. TRANSPORT

Above we found that the geometry of the molecule (connectivity of the redox orbitals) and the strong charging effects led to maximal spin states for $n=3,5$ extra electrons whereas for $n=2,4,6$ the spin is zero. We can restrict our attention to the transport in the bias and gate voltage regimes where these states are important. This is highlighted in the sketch of the conductance map by the circles in Fig. 7. Due to approximate electron-hole symmetry with respect to the

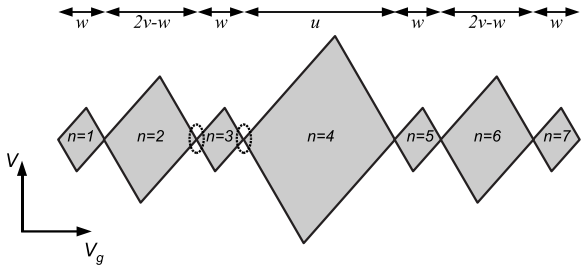

FIG. 7. Sketch of the $dI/dV(V_{\mathrm{g}}, V)$ map as function of gate V_{g} and bias voltage V. The current is suppressed inside the Coulomb diamonds. Their size scales with the various charging energies. The suppression is due to energy and charge quantization on the molecule. The circles indicate the gate and bias voltage regime where we demonstrate the fingerprints of the Nagaoka state (Figs. 8 and 9), not shown here.

$n=4$ state (cf. Fig. 4) we only need to consider $n=2,3,4$. We can also restrict our attention to the simpler model for the Fe grid described by Eq. (9) which captures all the basic effects.

The charge sensitivity of the total spin is observable in the single-electron tunneling current through the molecule.[32] To find the precise fingerprints of the Nagaoka effect in the transport and the role of the spin excitations in adjacent charge states of the molecule, we consider the Hamiltonian $H=H_{\mathrm{res}}+H_{\mathrm{Fe}}^{\mathrm{eff}}+H_{\mathrm{mol\text{-}res}}$, employing units $\hbar=e=k_B=1$. The electrodes $r=L,R$ are described as electron reservoirs with electrochemical potentials $\mu_r=\mu \pm V/2$ and a constant density of states ρ: $H_{\mathrm{res}}=\Sigma_{k\sigma r}\epsilon_{k\sigma r}c_{k\sigma r}^{\dagger}c_{k\sigma r}$. The tunneling term $H_{\mathrm{mol\text{-}res}}=(\Gamma/2\pi\rho)^{1/2}\Sigma_{k\sigma jr}t_j^r c_{k\sigma r}^{\dagger}a_{j\sigma}+\mathrm{H.c.}$ describes charge transfer between electrode and molecule (symmetric tunneling barriers). Γ is the overall coupling strength between leads and the molecule and defines the current scale. We assume that tunneling is only possible through two "contact" ligands, namely, $t_1^L=t_3^R=1$, otherwise 0. We have checked that this choice does not cause effects due to orbital symmetry as discussed in Ref. 15 by trying also $t_1^L=t_2^R=1$. The coupling to a gate electrode is included in a linear shift of the orbital energies. As above, the bias and gate energies are also expressed in units of the intramolecular tunneling $t=1$ which is connected to the effective hopping $T=t^2/(2\Delta)$. In the weak tunneling regime, Γ is much smaller than the temperature, the effect of the leads can be incorporated in the transition rates $\Sigma_{s,s'}=\Sigma_r\Sigma_{s,s'}^{r,+}+\Sigma_{s,s'}^{r,-}$ between the molecular many-body states s,s':

$$\Sigma_{s,s'}^{r,+}=\Gamma\sum_{\sigma} f_r^{+}(E_s-E_{s'})\left|\sum_j t_j^r\langle s|a_{j\sigma}^{\dagger}|s'\rangle\right|^2,$$

$$\Sigma_{s,s'}^{r,-}=\Gamma\sum_{\sigma} f_r^{-}(E_s-E_{s'})\left|\sum_j t_j^r\langle s|a_{j\sigma}|s'\rangle\right|^2. \qquad (12)$$

Here f_r^{+} is the Fermi function of reservoir r and $f_r^{-}=1-f_r^{+}$. Importantly, the matrix elements include the calculated many-body wave function of the molecule and the spin selection rules. From the stationary master equation $\Sigma_{s'}(\Sigma_{s,s'}P_{s'}-\Sigma_{s',s}P_s)=0$ we obtain the nonequilibrium occupations P_s of the molecular states s and the resulting stationary current which may be calculated at either electrode $r=L,R$:

$$I_r=-\sum_{s,s'}(\Sigma_{s,s'}^{r,+}P_{s'}-\Sigma_{s',s}^{r,-}P_s). \qquad (13)$$

Due to the presence of a maximal spin state, either as ground or excited state, spin blockade and NDC effects occur, respectively.[32]

Maximal spin ground state. For $u>u_{\mathrm{th}}$ and fixed t the ground state for $n=3,5$ is a Nagaoka state (Fig. 5). Transport involving ground states $n \leftrightarrow n+1$ for $n=2,\ldots,5$ is completely blocked for small bias and low temperature below the spin gap $|\Delta E|$: In the map of the differential conductance versus (V_g, V),[43] the Coulomb diamonds do not close (see Fig. 8). Since the ground-state spin is either 0 ($n=2,4,6$) or 3/2 ($n=3,5$) the tunneling rates between neighboring

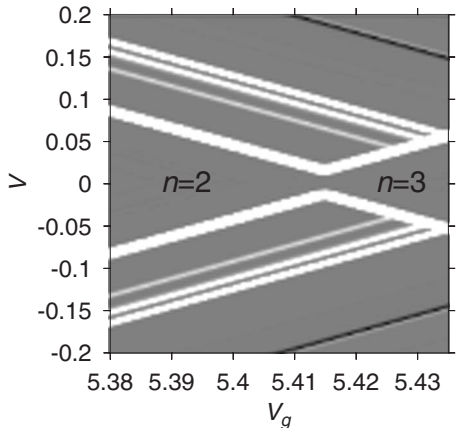

FIG. 8. $dI/dV(V_g,V)$ gray-scale plot [white (black) $>$ ($<$) 0] for $u=5$, $v=2.25$, $w=1$, $\Delta=-10$, temperature 2×10^{-4}.

ground states vanish due to the spin selection rule $|\Delta S|=1/2$ incorporated in Eq. (12). Even though the ground-state transitions are energetically allowed, transport is completely blocked in the weak tunneling limit. However, when the temperature or voltage is increased, such that the first excited state with appropriate spin can be accessed, current begins to flow.

Maximal spin excited state. Depending on the gate voltage, NDC and even complete current blocking can occur at finite bias voltage[32] when the Nagaoka state is the lowest spin excitation for $n=3,5$ (i.e., $u\lesssim u_{\text{th}}$; Fig. 5). The conductance fingerprint is shown in Fig. 9: near the charge $3\leftrightarrow4$ degeneracy point two NDC lines (black) with negative slope appear which are due to the low-lying $n=3$, $S=3/2$ Nagaoka state. We first discuss the lower NDC line using the left scheme in Fig. 10. At the charge degeneracy point ($V_g\sim6.58$ in Fig. 9) the current sets on because a transport channel is opened, namely, $n=3$, $S=1/2$ (orbital degenerate) $\leftrightarrow n=4$, $S=0$. Increasing the bias voltage by an amount Δ_4 ($n=4$ excitation energy; See Fig. 10) increases the population of the Nagaoka state via the $n=4$, $S=1$ excited state. Since the Nagaoka state cannot decay (strictly) to the $n=4$, $S=0$ ground state the number of transport channels is therefore decreased from two to one, leading to the lower NDC effect.

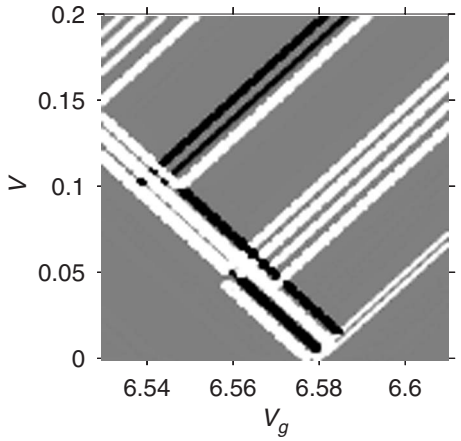

FIG. 9. Same parameters as Fig. 8 except $u=4.05$ and around a different charge degeneracy point.

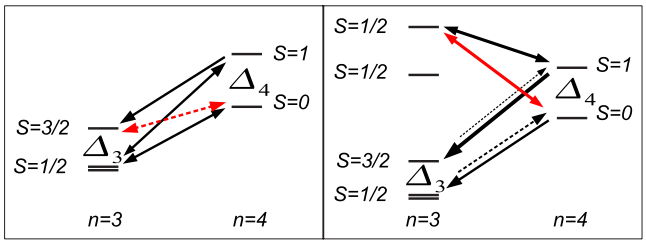

FIG. 10. (Color online) Left: minimal set of states for the lower NDC effect in Fig. 9 [spin-forbidden transition, dashed red (gray) line]. Right: minimal set of states for the complete current suppression in Fig. 9. The red (gray) line indicates the transition that opens the cascade.

Further away from the degeneracy point ($V_g\lesssim6.56$ in Fig. 9), the lower NDC line turns into a conductance peak and simultaneously the ground-state transition line below it disappears. This is due to a complete population inversion for $n=3$ between the ground ($S=1/2$) and excited ($S=3/2$) states which already occurs inside the Coulomb blockade region: when the transition from $n=4$, $S=0$ to the third excited state $n=3$, $S=1/2$ lies in the transport window, the Nagaoka state is occupied starting from the ground state $n=3$, $S=1/2$ via the cascade of single-electron tunneling processes indicated in the right panel of Fig. 10. We note that the second excited state of $n=3$ only couples to higher excited states of $n=4$ due to the symmetric connection to the electrodes chosen here. However, we have checked that it is not essential to the inversion mechanism. The Nagaoka state is fully occupied because the escape rate from $n=3$, $S=3/2$ relative to that from the $n=3$, $S=1/2$ ground state is suppressed by a factor $\sim e^{-(\Delta_4-\Delta_3)/T}\ll1$ (Fig. 10).

The upper NDC line with negative slope in Fig. 9 is caused by the occupation of a high-lying maximal spin state $n=4$, $S=2$ (not shown in Fig. 10) which cannot decay to states with one electron less and higher spin.[32] Only due to the presence of the low-lying Nagaoka state $S=3/2$ at $n=3$ can this state already be reached at such low voltages.

V. CONCLUSION

We have analyzed a strongly correlated electron model for a $[2\times2]$-grid complex to illustrate the interplay between electron addition and intramolecular spin coupling. We showed that low-temperature electron tunneling experiments can access the change of the molecular spin as a function of added charge and even the role of high-spin excitations in subsequent charge states. Our model contains both localized magnetic moments and delocalized electrons, in contrast to the customary description of molecular magnets. We have based our model on the addition energy spectra,[11] the crucial input being that the extra electrons occupy ligand orbitals. Due to the Nagaoka mechanism the total spin of the molecule is changed drastically upon variation of the total electron number. The charging energies on the ligands can be tuned chemically to the required large values for the

high-spin states by attaching electron-donating groups to the ligands. For a grid complex with localized spins on the mediating metal ions (Co) the total spin in the Nagaoka state is more than twice as large as for the Fe-grid complex. The direct exchange coupling of these spins with the neighboring ligands cooperates with the Nagaoka effect, by counteracting superexchange processes with the ligands and thereby further stabilizing the high-spin state.

We emphasize that other molecular complexes may also show the above behavior if the connectivity condition[27,35] of the electron-accepting centers is appropriate for the Nagaoka mechanism to be effective.

ACKNOWLEDGMENTS

J. Kortus is acknowledged for many stimulating discussions. We thank J.-M. Lehn for providing us experimental data and for discussions. M.R.W. acknowledges the financial support provided through the European Community's Research Training Networks Program under Contract No. HPRN-CT-2002-00302, Spintronics. W.W. acknowledges the support of the DFG (Grant No. WE 1863/14-1) as well as the use of computational facilities at the NIC supercomputer center. W.W. and H.S. acknowledge support by the Volkswagen Stiftung and the DFG (SPP 1337; SCHO 641/3-1).

[1] M. Ruben, J. Rojo, F. Romero-Salguero, L. Uppadine, and J.-M. Lehn, Angew. Chem., Int. Ed. **43**, 3644 (2004).
[2] L. Zhao, C. Matthews, L. Thomson, and S. Heath, Chem. Commun. (Cambridge) **4**, 265 (2000).
[3] M. Ruben, E. Breuning, J.-P. Gisselbrecht, and J.-M. Lehn, Angew. Chem., Int. Ed. **39**, 4139 (2000).
[4] O. Waldmann, L. Zhao, and L. K. Thompson, Phys. Rev. Lett. **88**, 066401 (2002).
[5] O. Waldmann, S. Carretta, P. Santini, R. Koch, A. G. M. Jansen, G. Amoretti, R. Caciuffo, L. Zhao, and L. K. Thompson, Phys. Rev. Lett. **92**, 096403 (2004).
[6] T. Guidi *et al.*, Phys. Rev. B **69**, 104432 (2004).
[7] O. Waldmann, Phys. Rev. B **71**, 094412 (2005).
[8] M. S. Alam, S. Strömsörfer, V. Dremov, P. Müller, M. Ruben, and J.-M. Lehn, Angew. Chem., Int. Ed. **44**, 7896 (2005).
[9] O. Waldmann, J. Hassmann, P. Müller, G. S. Hanan, D. Volkmer, U. S. Schubert, and J.-M. Lehn, Phys. Rev. Lett. **78**, 3390 (1997).
[10] O. Waldmann, M. Ruben, U. Ziener, and J.-M. Lehn, Inorg. Chem. **45**, 6535 (2006).
[11] M. Ruben, E. Breuning, M. Barboui, J.-P. Gisselbrecht, and J.-M. Lehn, Chem.-Eur. J. **9**, 291 (2003).
[12] E. Breuning, M. Ruben, J.-M. Lehn, F. Renz, Y. Garcia, V. Ksenofontov, P. Gütlich, E. Wegelius, and K. Rissanen, Angew. Chem., Int. Ed. **39**, 2504 (2000).
[13] M. Ruben, E. Breuning, J.-M. Lehn, V. Ksenofontov, F. Renz, P. Gütlich, and G. Vaughan, Chem.-Eur. J. **9**, 4422 (2003).
[14] A. A. Vlček, Coord. Chem. Rev. **43**, 39 (1982).
[15] M. H. Hettler, W. Wenzel, M. R. Wegewijs, and H. Schoeller, Phys. Rev. Lett. **90**, 076805 (2003).
[16] H. Park, J. Park, A. K. L. Lim, E. H. Anderson, A. P. Alivisatos, and P. L. McEuen, Nature (London) **407**, 57 (2000).
[17] J. Park *et al.*, Nature (London) **417**, 722 (2002).
[18] W. Liang, M. P. Shores, M. Bockrath, J. R. Long, and H. Park, Nature (London) **417**, 725 (2002).
[19] A. N. Pasupathy *et al.*, Nano Lett. **5**, 203 (2005).
[20] H. B. Heersche, Z. de Groot, J. A. Folk, H. S. J. van der Zant, C. Romeike, M. R. Wegewijs, L. Zobbi, D. Barreca, E. Tondello, and A. Cornia, Phys. Rev. Lett. **96**, 206801 (2006).
[21] H. S. J. van der Zant *et al.*, Faraday Discuss. **131**, 347 (2006).
[22] M.-H. Jo, J. E. Grose, M. M. Deshmukh, J. J. S. M. Rumberger, D. N. Hendrickson, J. R. Long, H. Park, and D. C. Ralph, Nano Lett. **6**, 2014 (2006).
[23] L. H. Yu and D. Natelson, Nanotechnology **15**, S517 (2004).
[24] L. H. Yu and D. Natelson, Nano Lett. **4**, 79 (2004).
[25] L. H. Yu, Z. K. Keane, J. W. Ciszek, L. Cheng, M. P. Stewart, J. M. Tour, and D. Natelson, Phys. Rev. Lett. **93**, 266802 (2004).
[26] Y. Nagaoka, Phys. Rev. **147**, 392 (1966).
[27] H. Tasaki, Prog. Theor. Phys. **99**, 489 (1998).
[28] J.-M. Lehn, *Supramolecular Chemistry: Concepts and Perspectives* (VCH, Weinheim, 1995).
[29] R. Arita, Y. Suwa, K. Kuroki, and H. Aoki, Phys. Rev. Lett. **88**, 127202 (2002).
[30] P. Huai, Y. Shimoi, and S. Abe, Phys. Rev. Lett. **90**, 207203 (2003).
[31] A. Izuoka, M. Hiraishi, T. Abe, T. Sugawara, K. Sato, and T. Takui, J. Am. Chem. Soc. **122**, 3234 (2000).
[32] D. Weinmann, W. Häusler, and B. Kramer, Phys. Rev. Lett. **74**, 984 (1995).
[33] C. Romeike, M. R. Wegewijs, W. Hofstetter, and H. Schoeller, Phys. Rev. Lett. **96**, 196601 (2006).
[34] C. Romeike, M. R. Wegewijs, and H. Schoeller, Phys. Rev. Lett. **96**, 196805 (2006).
[35] M. Kollar, R. Strack, and D. Vollhardt, Phys. Rev. B **53**, 9225 (1996).
[36] J. R. Schrieffer and P. A. Wolff, Phys. Rev. **149**, 491 (1966).
[37] W. Häusler, in *Advances in Solid State Physics* (Springer, Heidelberg, 1994), Vol. 34, 171.
[38] T. Kuzmenko, K. Kikoin, and Y. Avishai, Phys. Rev. B **69**, 195109 (2004).
[39] K. Kikoin and Y. Avishai, Phys. Rev. B **65**, 115329 (2002).
[40] J. B. Torrance, J. E. Vazquez, J. J. Mayerle, and V. Y. Lee, Phys. Rev. Lett. **46**, 253 (1981).
[41] S. Ishihara, T. Egami, and M. Tachiki, Phys. Rev. B **49**, 8944 (1994).
[42] H. Tasaki, Phys. Rev. B **40**, 9192 (1989).
[43] L. Kouwenhoven, C. Marcus, P. McEuen, S. Tarucha, R. Westervelt, and N. Wingreen, in *Mesoscopic Electron Transport*, edited by, L. L. Sohn, G. Schon, and L. P. Kouwenhoven, NATO Advanced Study Institute, Series B: Physics (Kluwer, Dodrecht, 1997).